Materials Science

AIMS Materials Science, 10(5): 934–947.
DOI: 10.3934/matersci.2023050
Received: 04 September 2023
Revised: 27 September 2023
Accepted: 08 October 2023
Published: 24 October 2023

http://www.aimspress.com/journal/Materials

Research article

Investigation on the effect of technological parameters of electrolyte-plasma cementation method on phase structure and mechanical properties of structural steel 20X

Bauyrzhan Rakhadilov[1,2], Lyaila Bayatanova[2], Sherzod Kurbanbekov[3,*], Ravil Sulyubayev[4], Nurdaulet Shektibayev[3] and Nurbol Berdimuratov[1]

[1] Research Center Surface Engineering and Tribology, Sarsen Amanzholov East Kazakhstan University, Ust-Kamenogorsk 070000, Kazakhstan
[2] Plasma Science LLP, Ust-Kamenogorsk 070000, Kazakhstan
[3] Department of Physics, Khoja Akhmet Yassawi International Kazakh-Turkish University, Turkestan 161200, Kazakhstan
[4] Scientific and Technical Center Vostoktehnoservis LLP, Ust-Kamenogorsk 070000, Kazakhsta

* **Correspondence:** Email: sherzod.kurbanbekov@ayu.edu.kz; Tel: +7-702-400-34-88.

Abstract: This article presents the results of a study on the effect of electrolyte-plasma cementation on the phase composition of the surface-modified layer and the mechanical properties of 20X steel using different solutions. It has been determined that electrolyte-plasma cementation followed by quenching in solutions containing (a) 10% calcined soda (Na_2CO_3), 10% urea (CH_4N_2O), 10% glycerin ($C_3H_8O_3$) and 70% distilled water and (b) 10% calcined soda (Na_2CO_3), 20% urea (CH_4N_2O) and 70% distilled water, results in the formation of a modified structure on the surface of 20X steel. This structure mainly consists of the α-Fe phase, along with separate particles of reinforcing phases, Fe_3C and Fe_3C_7 carbides and martensitic α′-Fe phase. The plasma of the electrolyte was used to heat the samples. Then these samples were partially immersed in the electrolyte and held at a temperature of 950 °C for 5 min, followed by quenching. As a result of this process, it was found that 20X steel exhibits higher hardness. After the electrolyte plasma cementation, it was observed that the friction coefficient of the modified surface of the steel samples significantly decreased. Additionally, the wear volume was reduced by more than 6.5 times compared to the initial state. The average microhardness after the electrolyte-plasma cementation is 660 HV, which is nearly four times higher than that of the initial material.

Keywords: electrolyte-plasma cementation; electrolyte composition; modified surface; microhardness; wear resistance

1. Introduction

One of the main tasks of the modern stage of mechanical engineering and industry development is the creation of energy and resource-saving technologies, improving the quality, reliability and durability of working sections of the parts and assemblies of various machines and mechanisms. Among the methods of surface hardening, the most common are surface thermal hardening and various methods of chemical-thermal treatment (cementation, nitrocarburization, nitriding, etc.). A promising and reliable trend for improving the quality of metal surfaces with the subsequent production of strengthening and protective coatings is high-rate electrolyte-plasma treatment followed by hardening in an aqueous electrolyte. Heating in the electrolyte plasma allows for a number of processes of local accelerated thermal and chemical-thermal treatment of steel parts as a result of a favorable combination of high temperature, active electrode and the flow of electrical discharges in a vapor-gas jacket between the metal being processed and the electrolyte [1–3]. These processes include heat treatment followed by cooling in the same electrolyte, carburization, nitrocarburization, nitriding and other types of complex diffusion saturation. The main advantages of high-rate electrolyte-plasma processing with subsequent hardening in an aqueous electrolyte are high processing rate, the absence of aggressive and toxic reagents and that the technology is implemented mainly in inexpensive solutions of neutral salts [4]. It is obvious that this method does not create residual stresses on the surface of the product. At the current state, the processing modes and electrolyte compositions for electrolyte-plasma cementation of various metals and alloys have been well developed and some physical and chemical features of the technology have been clarified [5]. At the same time, many basic issues of the process remain unexplored. These include the role of electrical discharges and electrochemical dissolution in removing materials from the surface of the processed part, the nature of the current passing through the vapor-gas layer, the properties and conditions of forming a surface oxide film, etc. Many hypotheses on the nature of the discharge in the vapor-gas jacket have been published, where it is called glowing [6], sparkling, arc and even streamer without any experimental evidence [7]. Knowledge of the qualitative and quantitative regularities of the formation of structural and phase states during the cementation is the basis for improving the technologies of chemical-thermal treatment, increasing the wear resistance and strength of machine parts subjected to high loads [8–10]. Unlike other types of heat treatment, the structural and phase transformations during thermo-cyclic and chemical-thermo-cyclic treatment are performed repeatedly with changing heating-cooling temperatures [11]. The need for repeated treatment is usually due to the desire to accumulate the changes that radically improve the quality of products and give them properties that are not achievable with a single thermal treatment [12–14]. It is known that the surface condition largely determines the level strength and operational properties of parts. It is the surface of the product that experiences increased wear, contact loads and is most of all affected by corrosion [15,16]. Surface hardening technologies, specifically the electrolyte-plasma hardening by physical and chemical methods, are based on a modifying effect on the steel surface, which radically changes its structure and practical properties [17]. Of all types of the electrolyte-plasma hardening, the cementation improves a number of mechanical properties of the steel surface layer,

including its wear resistance. The formation of a modified layer in the electrolyte-plasma cementation is related to the concentration of charge carriers in the vapor-gas jacket or the solution surface layer. Therefore, the electrolyte composition is the most complex factor due to the changes in many characteristics of the system. The most studied compositions are aqueous solutions for anodic cementation, which is carried out at temperatures of 900–1000 °C. For this reason, the effect of ammonium chloride concentration on the heating temperature is characterized by the voltage required to heat it up to 950 °C. According to the experimental data obtained, the voltage required to reach the desired anode temperature of 900 °C decreases with an increase in the concentration of ammonium chloride. The compositions of electrolytes for electrochemical-thermal modification usually contain two components, one of which provides a sufficiently high electrical conductivity of the solution, while the other is a source of the diffusing element. The solution containing ammonium chloride as an electrically conductive component and glycerin as a carbon-containing component has gained the most popularity for anodic cementation. These substances are not expensive or toxic. In addition, glycerin in electrolytes is relatively slowly depleted both during cathodic [18] and anodic heating [19]. The goal of this work is to study the phase composition and mechanical properties of the modified layer of structural 20X steel after cementation in different electrolytes.

2. Materials and methods

The research was provided with the plate samples measuring 15 × 15 × 5 mm made from the rolled pond of 20X steel, which contains the following elements in mass percentage: 0.18 C, 0.28 Si, 0.93 Cr, 0.2 Ni, 0.7 Mn, 0.032 P, 0.023 S. The electrolyte-plasma cementation was conducted using a specific facility constructed by our team [20] as follows above.

First, the sample was heated at a voltage of 320 V and a current of 20–25 A for 5 s. The heating of the samples was done using the electrolyte plasma, with the samples partially immersed in it to a depth of 4–5 mm. Then, the voltage was reduced to 180 V, the current changed to 10–12 A and the samples were held at a temperature of 950 °C for 5 min. After that, they were quenched in a stream of cooled electrolyte with a temperature of 60 °C. The choice of electrolyte for the electrolyte plasma saturation is relatively simple; the electrolyte for cementation should consist of carbon containing organic compounds in a conductive solution, such as KCl or Na_2CO_3. Varius environmentally friendly organic compounds and plasma-thermal decomposition, which provide the necessary ions and/or atom of carbon/nitrogen can be applied using this method in contrast to the traditional methods using cyanides [21]. The resource of the electrolyte is one of the most important operational properties. It is evident that the depletion of the solution due to the evaporation of volatile components will be proportional not only to the processing duration but also to the surface area being processed, the heating temperature, etc. For this reason, the intensity of the electrolyte usage is characterized by the amount of electricity passed through the electrolyte per unit volume. As an example, the results of anodic cementation in a water solution originally containing 15% ammonium chloride and 8% acetone, according to [22], showed that the acetone concentration decreased from 0.074 to 0.011 g/mL after passing a charge of 83.4 A·h/L. Most compositions of electrolytes are developed for steel saturation with nitrogen and carbon. In addition to water, solvents such as glycerin, form amide and other organic substances have been proposed. The necessary high electrical conductivity for anodic heating is achieved by the presence of corresponding components in the solutions [23]. Therefore, the electrolytes intended for chemical-thermal treatment (HTO) should

contain substances that provide the presence of saturating components in the vapor-gas jacket. In some cases, various additives are present in the solutions to improve certain properties of the electrolyte. The required proportions for the cementation solution are as follows:

- 10% calcined soda (Na_2CO_3), 20% glycerin ($C_3H_8O_3$), 70% distilled water;
- 10% calcined soda (Na_2CO_3), 10% urea (CH_4N_2O), 10% glycerin (CH_4N_2O), 70% distilled water;
- 10% calcined soda (Na_2CO_3), 20% urea (CH_4N_2O), 70% distilled water.

The temperature of the electrolyte was maintained at 55 ± 5 °C at the entrance to the operating chamber. The heating temperature was measured using a digital temperature meter ATE-9380.

The experimental research was conducted at the scientific research center Surface Engineering and Tribology of S. Amanzholov East Kazakhstan University (Ust-Kamenogorsk, Kazakhstan). The phase composition was determined using an X'PertPro X-ray diffractometer (Philips, Netherlands) with Cu-Kα radiation at 40 kV and 30 mA, with scanning parameters set at $35° < 2\theta < 85°$ with a step of 0.02° and a dwell time of 5 s. Data processing and quantitative analysis were performed using the PowderCell 2.4 software. The microstructure of the samples was revealed by chemical etching with a 4% solution of nitric acid (HNO_3) in ethyl alcohol. This reagent has been proposed for long time and is one of the most widely used in metallographic practice [24]. The microstructure examination was conducted using Altami 5C optical metallographic microscope (Russia) in reflected light under bright-field conditions. A scanning electron microscope (SEM) (TESCAN MIRA) was used to study the structure at ×4000 and ×10000 magnifications. The thickness of the diffusion zone, which had a clear boundary with the hardened sub-layer and the thickness of the hardened zone were evaluated based on the microstructure images of the cross-section and by analyzing the depth distribution of microhardness. The microhardness testing on the sample depth was carried out using a Vickers micro-hardness tester (Metolab 502, Russia) equipped with a diamond indenter and a load sensor up to 1000 g. The nanohardness tester (Nanoscan 4D Compact, Russia) equipped with a Berkovich diamond indenter, which has a three-sided pyramidal shape with a nominal angle of 65.3° and a diameter of 200 nm, was used to determine the hardness and elastic modulus using a load of 200 mN and a dwell time of 10 s during the testing. Five test series were conducted for each sample, and the obtained values were averaged to obtain the final value.

The steel tribological characteristics were measured in sliding friction mode using the "ball-disk" configuration on an Anton Paar TRB3 tribometer. The sample rotation speed was 2 cm/s, the load was 6 N and a Si_3N_4 (silicon nitride) ball with a diameter of 6 mm was used as a counterbody.

3. Results and discussion

By now, noteworthy results of cathodic and anodic variants of the electrolyte-plasma saturation of steels with carbon, boron and nitrogen have been published. The duration of the process for metals and alloys usually varies from 3–4 to 7–15 min. Increasing the duration of the process beyond these limits for the purpose of increasing the thickness of the hardened layer is unjustified, as it significantly increases energy costs, the amount of plasma dissolution of the part, reduces the resource of the working electrolyte and causes the method to lose its advantages in terms of rapid hardening and other competitive benefits over radiation heating in furnaces or other technological processes [25]. The results of studying the samples before and after the electrolytic plasma cementation are shown in Figure 1.

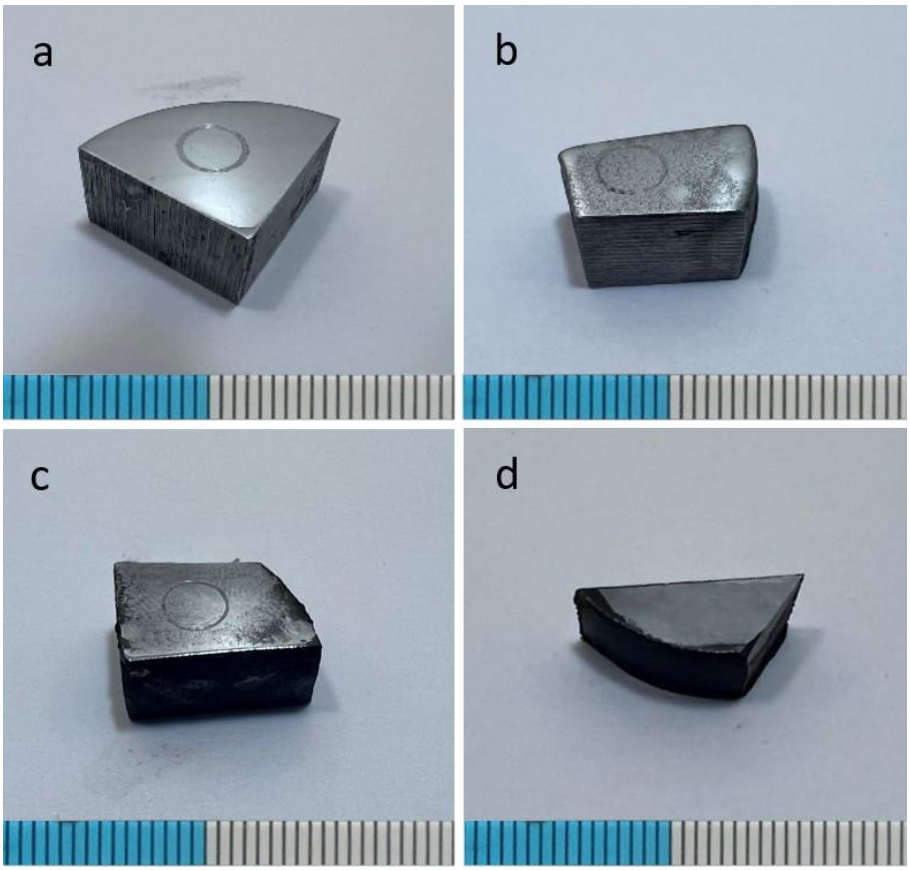

Figure 1. Appearance of 20X steel, (a) initial state, (b–d) after electrolytic-plasma cementation in different electrolyte compositions: (b) 10% Na_2CO_3 (calcined soda), 20% $C_3H_8O_3$ (glycerin), 70% distilled water; (c) 10% Na_2CO_3 (calcined soda), 10% CH_4N_2O (urea), 10% $C_3H_8O_3$ (glycerin), 70% distilled water; (d) 10% Na_2CO_3 (calcined soda), 20% CH_4N_2O (urea), 70% distilled water.

From the data of scanning electron microscopy, it can be seen that in the electrolyte containing 10% Na_2CO_3 (calcined soda), 20% CH_4N_2O (urea), and 70% distilled water, used for the cementation of 20X steel, the thickness of the modified layer reaches 65 μm at 950 °C (Figure 2). Also, in Figure 2 the microstructure can be divided into 3 zones: (1) modified layer zone, (2) thermally affected zone and (3) zone having the original matrix structure. The transition zone exhibits a finer-grained structure, characteristic of the heat-affected zone, compared to the coarse-grained structure of the matrix. Elemental microanalysis showed the highest content of iron (98.1 wt.%), followed by carbon (0.9 wt.%), oxygen (0.3 at.%) and manganese (0.7 wt.%) in region 1 in Figure 2. In region 2, the content of carbon, oxygen and manganese decreases to 0.3, 0.1 and 0.3 wt.%, respectively. In region 3, significant changes in the content of diffusing elements were not observed. Thus, the analysis of the distribution of these diffusing elements showed that in the modified layer after processing, there is a higher content of carbon compared to oxygen. High rates of the electrolyte heating not only reduce the time to reach the required temperature of the part but also accelerate the formation of the diffusion layers [26]. The reason for this is the positive effect of heating conditions on certain elementary processes of the chemical-thermal treatment. Increasing the temperature is most effective, as the diffusion coefficient and reaction rate constants are exponentially dependent on it [27].

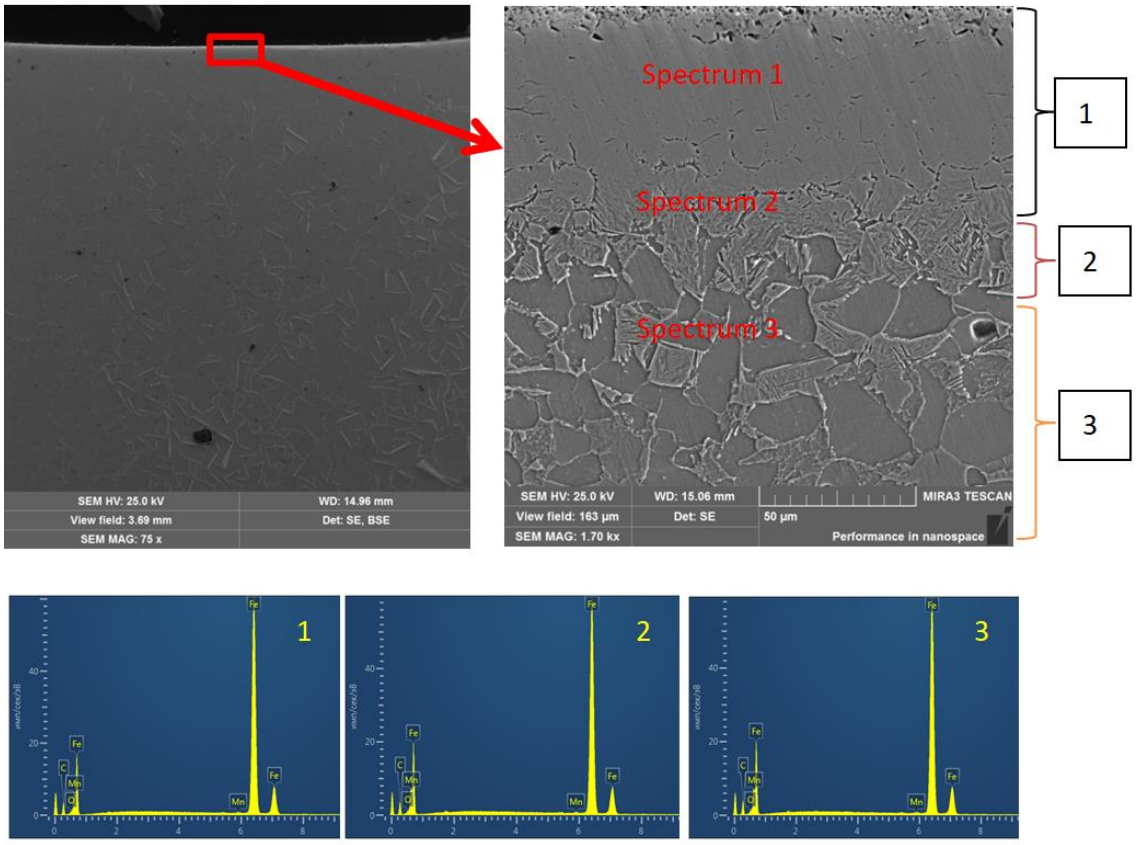

Figure 2. Elemental composition of the modified surface of 20X steel, processed in the electrolyte containing 10% Na_2CO_3 (calcined soda), 20% CH_4N_3O (urea) and 70% distilled water, according to energy-dispersive X-ray microanalysis data.

The phase composition of low-carbon steel cemented is determined by the composition of the vapor-gas jacket and the heating and cooling conditions of the part. After cathodic cementation with cooling in the solution, the surface layer may contain a cementite grid, martensite and residual austenite [28]. Figure 3 shows X-ray diffraction patterns indicating changes in the phase composition of the steel modified surface. It can be observed that after the electrolytic-plasma cementation, the phase composition of the samples includes strengthening phases Fe_3C, Fe_7C_3 (carbides), α′-Fe martensitic phase and residual α-Fe phase. Thus, with a change in the electrolyte composition, the width of the peaks of the martensitic α′-Fe phase and Fe_3C phase decreases. It has been determined that the changes in the phase composition of the modified layer primarily depend on the electrolyte composition. It is known that the most complex factor is the composition of the electrolyte—10% calcined soda (Na_2CO_3), 20% glycerin ($C_3H_8O_3$), 70% distilled water. A slight increase in the half-width of the diffraction lines can be observed in Figure 3a. The X-ray phase analysis of the samples processed in the electrolytes (10% calcined soda (Na_2CO_3), 10% urea (CH_4N_2O), 10% glycerin ($C_3H_8O_3$), 70% distilled water and 10% calcined soda (Na_2CO_3), 20% urea (CH_4N_2O), 70% distilled water) are quite similar to each other and are characterized by the identification of the following formed phases Fe_3C, Fe_7C_3 and martensitic α′-Fe phase (Figure 3b,c). An increase in the half-width of the diffraction lines, including the average intensity, is observed. It is known [29,30] that broadening of the diffraction peaks is contributed by changes in the crystalline structure such as:

the presence of crystals with different compositions in the X-rayed volume, within the range of the homogeneity region with the corresponding range of variations in interplanar distance; consequences of "cold" deformation, in the form of residual stresses, multiple deformation packing defects and mosaic block fragmentation; when the dissolved substances are nonuniformly distributed in a solid solution, elastic concentration stresses arise due to changes in the lattice constant during the incorporation of dissolved atoms. Therefore, the observed broadening of the diffraction lines can be attributed to the incorporation of carbon atoms into the crystalline structure based on the martensitic α′-Fe phase. The phase composition of the modified layer obtained in the electrolyte with the composition of 10% calcined soda (Na_2CO_3), 20% urea (CH_4N_2O) and 70% distilled water slightly differs from the electrolyte that contains glycerin. The results of the phase composition analysis of 20X steel are consistent with the data obtained by other researchers [31] and suggest an increase in the physical and mechanical properties of the synthesized coatings not only due to the high content of alloying additives of refractory metals but also due to the amorphous structure.

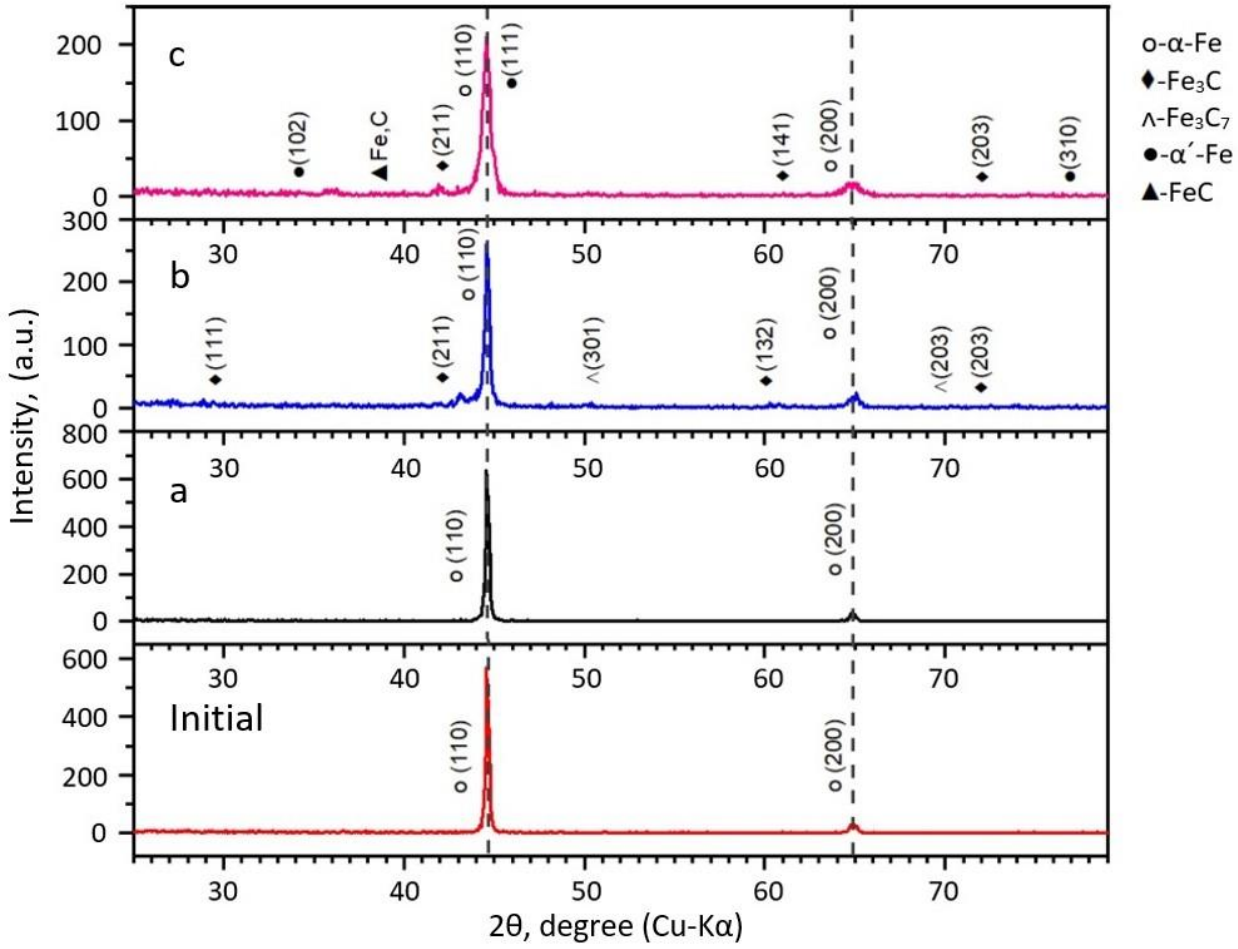

Figure 3. Diffraction patterns of 20X steel modified layer after electrolytic-plasma cementation in different electrolyte compositions: (a) 10% Na_2CO_3 (calcined soda), 20% $C_3H_8O_3$ (glycerin), 70% distilled water; (b) 10% Na_2CO_3 (calcined soda), 10% CH_4N_2O (urea), 10% $C_3H_8O_3$ (glycerin), 70% distilled water; (c) 10% Na_2CO_3 (calcined soda), 20% CH_4N_2O (urea), 70% distilled water.

Microhardness is one of the most important characteristics that can be used to assess the operational properties of the modified surface [32]. The structure of the cemented layer can be characterized as martensitic with cementite grid nuclei on the part surface. The microhardness distribution in the modified layer corresponds to its phase composition and the electrolyte concentration. As Figure 4 shows, the microhardness values ranged from 221–660 HV. The maximum value was observed after processing at 900 °C in the electrolyte containing 10% Na_2CO_3 (calcined soda), 20% CH_4N_2O (urea), 70% distilled water and amounted to 660 HV (Figure 4). The highest microhardness of the modified layer after the electrolytic-plasma cementation with subsequent quenching in the same electrolyte was likely due to the increase in the concentration of the saturating component, carbon and the quenching effect. Similar results were obtained by the authors of the study during cathodic cementation of samples with a diameter of 10 mm and a length of 40 mm, immersed in the electrolyte to a depth of 15 mm and containing 0.15% carbon. The composition of the electrolyte was a 25% solution of potassium acetate in glycerin [33]. Additionally, the possibility of increasing the heat resistance of low-carbon steel up to 900 °C through the electrolytic-plasma cementation was demonstrated [34]. Of course, other advantages of electrolytic-plasma diffusion saturation are preserved, such as high processing rate, reducing the saturation time to a few minutes and combining saturation with quenching without reheating.

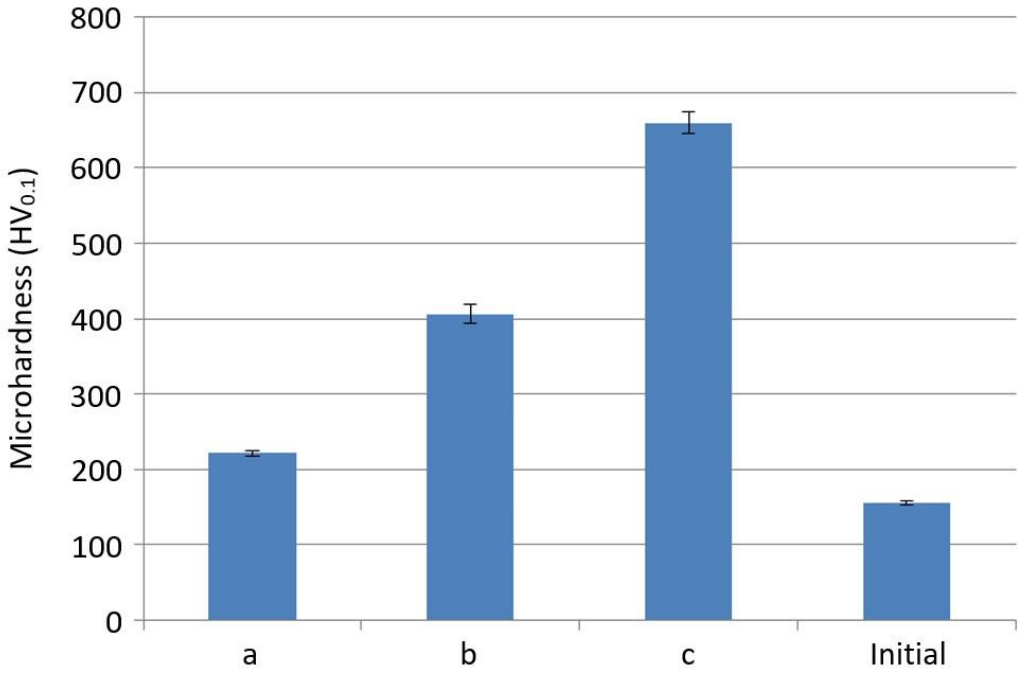

Figure 4. Surface microhardness of 20X steel samples after heating at 950 °C for 5 min followed by quenching in different electrolyte compositions: (a) 10% Na_2CO_3 (calcined soda), 20% $C_3H_8O_3$ (glycerin), 70% distilled water; (b) 10% Na_2CO_3 (calcined soda), 10% CH_4N_2O (urea), 10%, $C_3H_8O_3$ (glycerin), 70% distilled water; (c) 10% Na_2CO_3 (calcined soda), 20% CH_4N_2O (urea), 70% distilled water.

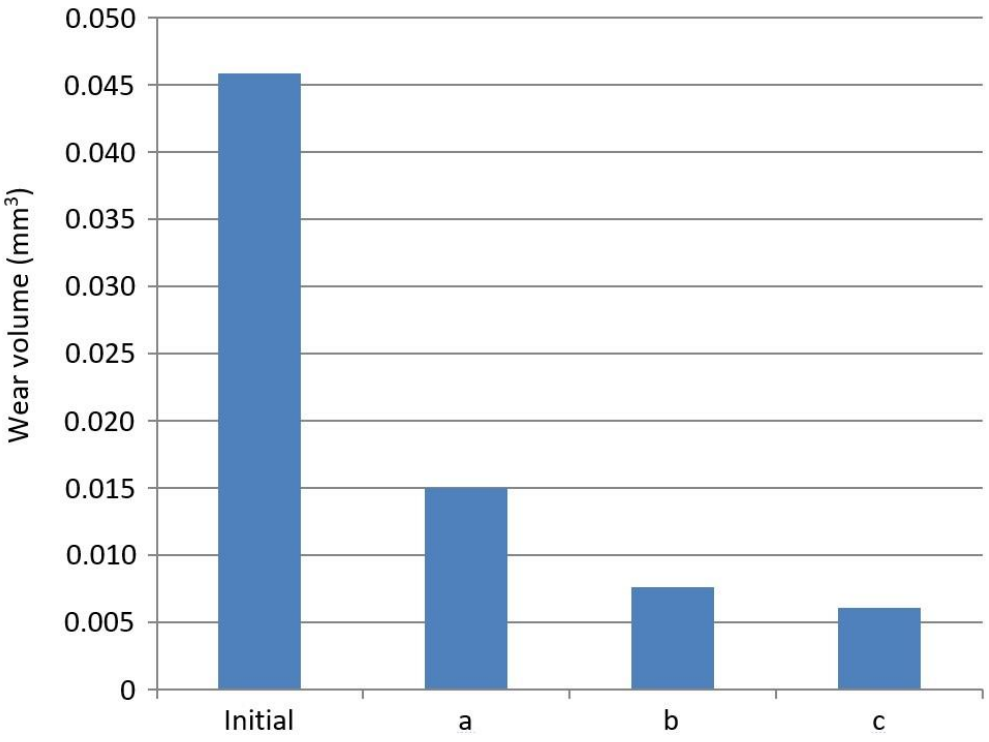

Figure 5. Wear volume of 20X steel samples after heating at 950 °C for 5 min followed by quenching in different electrolyte compositions: (a) 10% Na_2CO_3 (calcined soda), 20% $C_3H_8O_3$ (glycerin), 70% distilled water; (b) 10% Na_2CO_3 (calcined soda), 10% CH_4N_2O (urea), 10% $C_3H_8O_3$ (glycerin), 70% distilled water; (c) 10% Na_2CO_3 (calcined soda), 20% CH_4N_2O (urea), 70% distilled water.

Currently, the wear resistance of steels is determined by their high hardness. However, the structure of the surface layer that corresponds to maximum wear resistance and the structure corresponding to maximum hardness are not always the same. Wear resistance is a structurally sensitive characteristic. Therefore, it is not always necessary to strive for steel maximum hardness. During the friction, changes in the structure and properties of the material in the zone of the surface plastic deformation occur, creating a friction structure that controls the wear degree. In turn, the deformation zone structure during the friction depends on the layer initial structure. Thus, there is a relationship between the conditions of steel pre-treatment, which form a certain structural state of the surface layer, the conditions of the electrolytic-plasma cementation, which create a characteristic structural state of the modified layer and the tribotechnical characteristics of the structural state of the deformation zone during the friction. Determining this relationship is a key to solving the optimization task of the technological process of the electrolytic-plasma cementation for the materials and products intended for the tribotechnical purposes. The martensite nonuniform composition, caused by high heating rates and large internal stresses due to the rapid cooling, resulted in a fairly high wear resistance of 20X steel quenched in the electrolyte. Figure 5 shows the results of wear resistance testing of the samples hardened by various electrolyte compositions. The steel tribological characteristics were measured in the sliding friction mode according to the "ball-disk" scheme on Anton Paar TRB3 tribometer. The sample rotation speed was 2 cm/s, the load was 6 N and a ball of Si_3N_4 (silicon nitride) with a diameter of 6 mm was used as a counterbody.

The samples after the electrolytic-plasma cementation in different solutions containing 10% Na_2CO_3 (calcined soda), 20% CH_4N_2O (urea) and 70% distilled water, showed high wear resistance. The wear volume was about 6.5 times less than that of the original 20X steel samples. Studies [35] suggest that the electrolytic-plasma cementation, nitrocementation and nitriding followed by quenching increase the wear resistance of steel and titanium alloys. Performing two operations on the same installation allows for the significant reduction in the duration of the technological cycle and its cost.

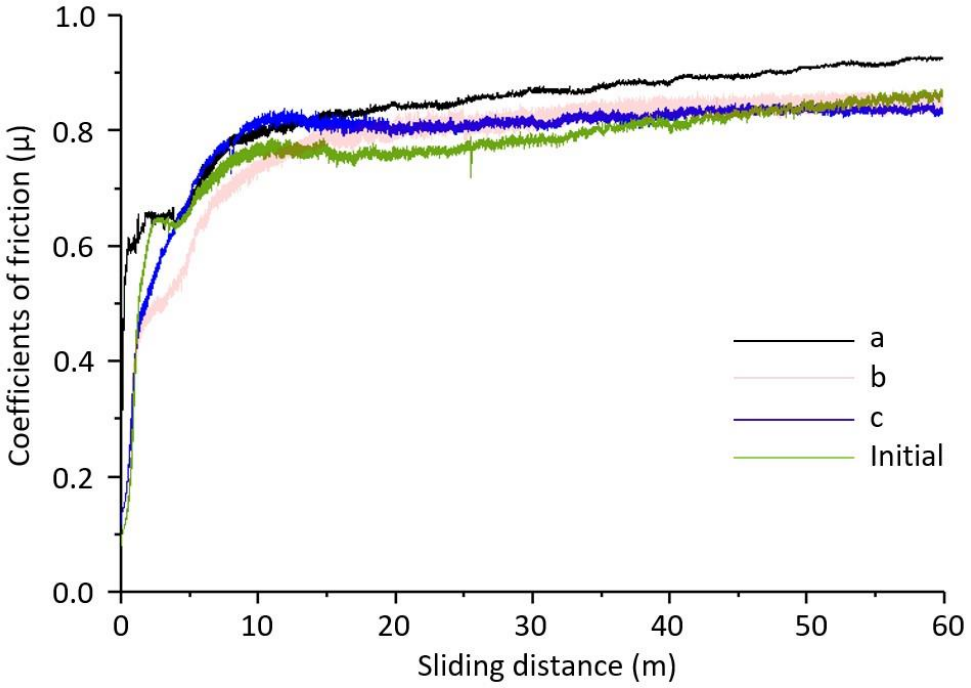

Figure 6. Friction coefficient of the modified surface of 20X steel samples after heating at 950 °C for 5 min followed by quenching in different electrolyte compositions: (a) 10% Na_2CO_3 (calcined soda), 20% $C_3H_8O_3$ (glycerin), 70% distilled water; (b) 10% Na_2CO_3 (calcined soda), 10% CH_4N_2O (urea), 10% $C_3H_8O_3$ (glycerin), 70% distilled water; (c) 10% Na_2CO_3 (calcined soda), 20% CH_4N_2O (urea), 70% distilled water.

The surface wear behavior, presented as a diagram of the friction coefficient dependence on the length of the indenter path, shows that the wear path can be divided into three segments: the running-in path (rapid increase in friction coefficient), the modified surface wear path (gradual increase in friction coefficient) and the base material wear path (section with a constant friction coefficient). From Figure 6, it was established that the tribological characteristics of the samples treated in different electrolyte compositions do not vary significantly from each other. In the as-received state, the friction coefficient of 20X steel is in the range of 0.67–0.89. Similarly, 20X steel treated in the electrolyte with 10% Na_2CO_3 (calcined soda), 20% $C_3H_8O_3$ (glycerin) and 70% distilled water, showed a stable friction coefficient of 0.81–0.97, while in the electrolyte with 10% Na_2CO_3 (calcined soda), 10% CH_4N_2O (urea), 10% $C_3H_8O_3$ (glycerin) and 70% distilled water, it showed a stable friction coefficient of 0.68–0.87. In the electrolyte with 10% Na_2CO_3 (calcined soda), 20% CH_4N_2O (urea) and 70% distilled water, the stable friction coefficient was in the range of 0.81–0.77. It can be observed that the difference between the ranges is small compared to the steel

treated in other electrolyte compositions. The significant reduction in the friction coefficient indicates a decrease in wear. These data are similar to those obtained in works [36,37], where the wear tests of the samples were conducted in Ringer's solution and under atmospheric conditions. It was shown that the electrolyte-plasma hardening resulted in a significant reduction in the friction coefficient. Ringer's solution acted as a lubricating material during the wear tests, leading to more even load distribution over the sample entire surface. The presence of Ringer's solution also contributed to a reduction in the friction coefficient compared to the tests conducted in normal atmosphere. The friction coefficient reached a minimum value of about 0.4 for the sample tested under atmospheric conditions and about 0.15 for the sample in Ringer's solution. This is 10 times lower than in untreated samples.

4. Conclusions

The electrolyte-plasma cementation of steels in aqueous electrolytes represents a relatively new trend of the method. The obtained results cover the main aspects of metallurgy, such as the structure and phase composition of the modified layers, 4 processing modes and electrolyte compositions, microhardness and tribological properties of the treated materials. Some attention was paid to the electrochemical specifics of the cementation in electrolyte solutions, in particular cathodic dissolution, as well as the specifics of the deposition of the saturating component from boiling electrolyte and the transfer of the active saturating element to the treated surface. In this regard, it has been established that after the electrolyte-plasma cementation of the samples treated in an electrolyte with a composition of 10% calcined soda (Na_2CO_3), 10% urea (CH_4N_2O), 10% glycerin ($C_3H_8O_3$) and 70% distilled water and also 10% calcined soda (Na_2CO_3), 20% urea (CH_4N_2O) and 70% distilled water at a temperature of 950 °C for 5 min, the surface of 20X steel forms a modified structure, with the main composition represented by martensitic α'-Fe phase, as well as individual particles of strengthening phases, carbides Fe_3C and Fe_3C_7 and residual α-Fe phase. The appearance of new phases contributes to a significant strengthening of 20X steel modified surface. It has been found that 20X steel cementing with subsequent quenching can increase microhardness. The average microhardness after the electrolyte-plasma cementation is 660 HV, which is almost 4 times higher than the original material. It has been also found that after the electrolyte-plasma cementation, the friction coefficient of the modified surface of the steel samples significantly decreased and the wear volume decreased more than 6.5 times compared to the initial state. Of course, other advantages of electrolyte-plasma diffusion saturation are preserved, high processing rate, reducing the saturation duration to several minutes, combining saturation with quenching without reheating, convenience of local surface modification by partial immersion in electrolyte or jet heating and the absence of toxic substances and expensive equipment. Overall, the obtained results convincingly demonstrate the significant potential of the electrolyte-plasma cementation of steels not only for scientific research but also for industrial use. Therefore, further development of the method in promising trends is considered to be justified. It was established that the electrolyte-plasma cementation, nitrocementation and nitriding allow obtaining modified layers on 20X steel products with high physicomechanical properties. The possibility of increasing the surface hardness of the samples after the electrolyte-plasma cementation without reducing both general corrosion resistance and resistance to intergranular corrosion has been shown. The steel surface wear and corrosion resistance increase due to changes in the structural and phase state of the surface layer. The emergence of such structural

components as nitrides, carbides and needle-like martensite in the modified layers of 20X steel becomes possible due to the steel saturation with nitrogen and carbon during the electrolyte-plasma cementation.

Use of AI tools declaration

The authors declare they have not used Artificial Intelligence (AI) tools in the creation of this article.

Acknowledgments

This research is funded by the Science Committee of the Ministry of Science and Higher Education of the Republic of Kazakhstan (Grant No. AP09058547).

Conflict of interest

The authors declare no conflict of interest.

References

1. Mozafarnia H, Fattah-Alhosseini A, Chaharmahali R, et al. (2022) Corrosion, wear, and antibacterial behaviors of hydroxyapatite/MgO composite PEO coatings on AZ31 Mg alloy by incorporation of TiO_2 nanoparticles. *Coatings* 12: 1967. https://doi.org/10.3390/coatings12121967
2. Belkin PN, Yerokhin A, Kusmanov SA (2016) Plasma electrolytic saturation of steels with nitrogen and carbon. *Surf Coat Technol* 307: 1194–1218. https://doi.org/10.1016/j.surfcoat.2016.06.027
3. Zarchi MK, Shariat MH, Dehghan SA, et al. (2013) Characterization of nitrocarburized surface layer on AISI 1020 steel by electrolytic plasma processing in an urea electrolyte. *J Mater Res Technol* 3: 213–220. https://doi.org/10.1016/j.jmrt.2013.02.011
4. Belkin PN, Kusmanov SA (2021) Plasma electrolytic carburising of metals and alloys. *Surf Engin Appl Electrochem* 57: 19–50. https://doi.org/10.3103/S1068375521010038
5. Vana D, Podhorsky S, Hurajt M, et al. (2013) Surface properties of the stainless steel X10CrNi18/10 after aplication of plasma polishing in electrolyte. *Int J Mod Eng Res* 3: 788–792. Available from: https://citeseerx.ist.psu.edu/document?repid=rep1&type=pdf&doi=0cdd0bb9b826f3e02c4566636f3f2983dbb9b216.
6. Wu J, Deng J, Dong L, et al. (2023) Direct growth of oxide layer on carbon steel by cathodic plasma electrolysis. *Surf Coat Technol* 338: 63–68. https://doi.org/10.1016/j.surfcoat.2018.01.080
7. Das K, Sen S, Joseph A, et al. (2023) Investigation on the effects of pretreatment on the surface characteristics of duplex plasma-treated AISI P20 tool steel. *Materialia* 27: 101679. https://doi.org/10.1016/j.mtla.2023.101679

8. Ding H, Su CR, Wang WJ, et al. (2019) Investigation on the rolling wear and damage properties of laser discrete quenched rail material with different quenching shapes and patterns. *Surf Coat Technol* 378: 124991. https://doi.org/10.1016/j.surfcoat.2019.124991
9. Krit BL, Apelfeld AV, Borisov AM, et al. (2023) Plasma electrolytic modification of zirconium and its alloys: Brief review. *Materials* 16: 5543. https://doi.org/10.3390/ma16165543
10. Inoue M, Iwane H, Kikuyama H, et al. (2022) Preparation of highly ionic conductive lithium phosphorus oxynitride electrolyte particles using the polygonal barrel-plasma treatment method. *J Alloys Compd* 923: 166350. https://doi.org/10.1016/j.jallcom.2022.166350
11. Aliofkhazraei M, Rouhaghdam AS, Gupta P (2011) Nano-fabrication by cathodic plasma electrolysis. *Crit Rev Solid State* 36: 174–190. https://doi.org/10.1080/10408436.2011.593269
12. Monaca AL, Murray JW, Liao Z, et al. (2021) Surface integrity in metal machining-Part II: Functional performance. *Int J Mach Tool Manu* 164: 103718. https://doi.org/10.1016/j.ijmachtools.2021.103718
13. Molaei M, Alhosseini AF, Nouri M, et al. (2023) Role of TiO_2 nanoparticles in wet friction and wear properties of PEO coatings developed on pure titanium. *Metals* 13: 821. https://doi.org/10.3390/met13040821
14. Jin X, Wang B, Du J, et al. (2013) Characterization of wear-resistant coatings on 304 stainless steel fabricated by cathodic plasma electrolytic oxidation. *Surf Coat Technol* 236: 22–28. https://doi.org/10.1016/j.surfcoat.2013.04.056
15. Rakhadilov BK, Kurbanbekov SR, Kilishkhanov MK, et al. (2018) Changing the structure and phase states and the microhardness of the R6M5 steel surface layer after electrolytic-plasma nitriding. *Eurasian J Phys Funct Mater* 2: 259–266. https://doi.org/10.29317/ejpfm.2018020307
16. Jumbad VR, Chel A, Verma U, et al. (2020) Application of electrolytic plasma process in surface improvement of metals: A review *Lett Appl NanoBioScience* 9: 1249–1262. https://doi.org/10.33263/LIANBS93.12491262
17. Rakhadilov B, Satbayeva Z, Ramankulov S, et al. (2021) Change of 0.34Cr-1Ni-Mo-Fe steel dislocation structure in plasma electrolyte hardening. *Materials* 14: 1928. https://doi.org/10.3390/ma14081928
18. Bottgen-Hiller F, Nustler K, Zeidler H, et al. (2016) Plasma electrolytic polishing of metalized carbon fibers. *AIMS Mater Sci* 3: 260–269. https://doi.org/10.3934/matersci.2016.1.260
19. Alekseev YG, Korolyov AY, Niss VS, et al. (2016) Electrolytic-plasma treatment of inner surface of tubular products. *Sci Tech-Bel* 15: 61–68. https://doi.org/10.21122/2227-1031-2016-15-1-61-68
20. Zhurerova LG, Rakhadilov BK, Popova NA, et al. (2020) Effect of the PEN/C surface layer modification on the microstructure, mechanical and tribological properties of the 30CrMnSiA mild-carbon steel. *J Mater Res Technol* 9: 291–300. https://doi.org/10.1016/j.jmrt.2019.10.057
21. Yerokhin A, Nie X, Leyland A, et al. (1999) Plasma electrolysis for surface engineering. *Surf Coat Technol* 122: 73–93. https://doi.org/10.1016/S0257-8972(99)00441-7
22. Jiang Y, Geng T, Bao Y, et al. (2013) Electrolyte–electrode interface and surface characterization of plasma electrolytic nitrocarburizing. *Surf Coat Technol* 216: 232–236. https://doi.org/10.1016/j.surfcoat.2012.11.050
23. Jiang YF, Bao YF, Yang K (2012) Effect of C/N concentration fluctuation on formation of plasma electrolytic carbonitriding coating on Q235. *J Iron Steel Res Int* 19: 39–45. https://doi.org/10.1016/S1006-706X(13)60018-7

24. Novoselov MV, Schilling N, Rudavin A, et al. (2018) Assessment of the possibility of polishing stainless steels by jet electrolyte-plasma treatment. *Mater Sci* 20: 94–102.
25. Kalenchukova OV, Nagula P, Tretinnikov DL (2015) About changes in the chemical composition of the electrolyte in the process of electrolytic-plasma treatment of materials. *Mater Methods Technol* 9: 404–413.
26. Ayday A, Durman M (2013) Surface hardening of ductile cast iron by electrolytic plasma technology. *Acta Phys Pol* 123: 291–293. https://doi.org/10.12693/APhysPolA.123.291
27. Belkin PN, Ganchar VI, Davydov AD, et al. (1997) Anodic heating in aqueous solutions of electrolytes and their use for treating metal surface. *Surf Engin Appl Electrochem* 2: 1–15.
28. Pang H, Lv G, Chen H, et al. (2009) Microstructure and corrosion performance of carbonitriding layers on cast iron by plasma electrolytic carbonitriding. *Chinese Phys Lett 2*9: 086805. https://dx.doi.org/10.1088/0256-307X/26/8/086805
29. Denisenko A, Romanyuk A, Pietzka C, et al. (2010) Surface structure and surface barrier characteristics of boron-doped diamond in electrolytes after CF_4 plasma treatment in RF-barrel reactor. *Diam Relat Mater* 19: 423–427. https://doi.org/10.1016/j.diamond.2009.12.016
30. Pardo P, Bastid J, Serrano FJ, et al. (2009) X-ray diffraction line-broadening study on two vibrating, dry-milling procedures in kaolinites. *Clays Clay Miner* 57: 25–34. https://doi.org/10.1346/CCMN.2009.0570102
31. Cavuslu F, Usta M (2011) Kinetics and mechanical study of plasma electrolytic carburizing for pure iron. *Appl Surf Sci* 257: 4014–4020. https://doi.org/10.1016/j.apsusc.2010.11.167
32. Yang Y, Peng K, Deng Y, et al. (2022) The synthesis of nickel sulfide deposited with nitrogen-doped carbon quantum dots as advanced electrode materials for supercapacitors. *J Mater Sci* 57: 14052–14064. https://doi.org/10.1007/s10853-022-07513-0
33. Bayatanova L, Rakhadilov B, Kurbanbekov S (2021) Fine structure of low-carbon steel after electrolytic plasma treatment. *Mater Test* 63: 842–847. https://doi.org/10.1515/mt-2020-0119
34. Mukhacheva T, Kusmanov S, Suminov I, et al. (2022) Increasing wear resistance of low-carbon steel by anodic plasma electrolytic sulfiding. *Metals* 12: 1641. https://doi.org/10.3390/met12101641
35. Pogrebnyak AD, Kaverina AS, Kylyshkanov MK (2014) Electrolytic plasma processing for plating coatings and treating metals and alloys. *Prot Met Phys Chem Surf* 50: 72–87. https://doi.org/10.1134/S2070205114010092
36. Mukhacheva TL, Belkin PN, Dyakov IG, et al. (2020) Wear mechanism of medium carbon steel after its plasma electrolytic nitrocarburising. *Wear* 462–463: 203516. https://doi.org/10.1016/j.wear.2020.203516
37. Kazerooni NA, Bahrololoom ME, Shariat MH, et al. (2011) Effect of ringer's solution on wear and friction of stainless steel 316L after plasma electrolytic nitrocarburising at low voltages. *J Mater Sci Technol* 27: 906–912. https://doi.org/10.1016/S1005-0302(11)60163-1